

# OUTSTANDING MEETING PAPER

*Papers in this section are based on submissions to the MRS Symposium Proceedings that were selected by Symposium Organizers as the outstanding paper. Upon selection, authors are invited to submit their research results to Journal of Materials Research. These papers are subject to the same peer review and editorial standards as all other JMR papers. This is another way by which the Materials Research Society recognizes high quality papers presented at its meetings.*

## Review

### Phase field theory of crystal nucleation and polycrystalline growth: A review

L. Gránásy,<sup>a)</sup> T. Pusztai, T. Börzsönyi, G. Tóth, and G. Tegze  
*Research Institute for Solid State Physics and Optics, H-1525 Budapest, Hungary*

J.A. Warren and J.F. Douglas  
*National Institute of Standards and Technology, Gaithersburg, Maryland 20899*

(Received 17 June 2005; accepted 6 October 2005)

We briefly review our recent modeling of crystal nucleation and polycrystalline growth using a phase field theory. First, we consider the applicability of phase field theory for describing crystal nucleation in a model hard sphere fluid. It is shown that the phase field theory accurately predicts the nucleation barrier height for this liquid when the model parameters are fixed by independent molecular dynamics calculations. We then address various aspects of polycrystalline solidification and associated crystal pattern formation at relatively long timescales. This late stage growth regime, which is not accessible by molecular dynamics, involves nucleation at the growth front to create new crystal grains in addition to the effects of primary nucleation. Finally, we consider the limit of extreme polycrystalline growth, where the disordering effect due to prolific grain formation leads to isotropic growth patterns at long times, i.e., spherulite formation. Our model of spherulite growth exhibits branching at fixed grain misorientations, induced by the inclusion of a metastable minimum in the orientational free energy. It is demonstrated that a broad variety of spherulitic patterns can be recovered by changing only a few model parameters.

## I. INTRODUCTION

Most of our structural materials are polycrystalline, i.e., composed of a large number of crystallites, whose size, shape, and composition distributions determine their properties and failure characteristics. Polycrystalline patterns play an important role in classical materials science and nanotechnology and have biological relevance as well. Specifically, semi-crystalline spherulites of amyloid fibrils are found in association with Alzheimer and Creutzfeldt–Jakob diseases, type II diabetes, and a range of systemic and neurotic disorders.<sup>1</sup>

Despite intensive research, the formation of polycrystalline matter (technical alloys, polymers, minerals, etc.) is poorly understood. One of the sources of theoretical difficulty in modeling these materials is modeling the process of nucleation by which crystallites form via fluctuations. While nucleation takes place on the nanometer scale, its influence extends to larger size

scales. Controlled nucleation<sup>2</sup> is an established tool for tailoring the microstructure of matter for specific applications.

The crystallization of homogeneous undercooled liquids initiates by the formation of heterophase fluctuations containing a central, crystal-like atomic arrangement. Fluctuations that exceed a critical size, determined by the interplay of the interfacial and volumetric contributions to the cluster free energy, reach macroscopic dimensions with high probability, while clusters below the critical size decay with a high probability. Critical size heterophase fluctuations are termed “nuclei,” and the process in which they form via internal fluctuations of the liquid is homogeneous nucleation (as opposed with the heterogeneous nucleation, where particles, foreign surfaces, or impurities help to produce the heterophase fluctuations that drive the system towards solidification). Even in simple liquids (such as the Lennard–Jones model system), several local arrangements [body-centered cubic (bcc), face-centered cubic (fcc), hexagonal close-packed (hcp), icosahedral] compete,<sup>3,4</sup> and often a metastable phase nucleates.

The description of near-critical fluctuations is problematic even in one-component systems. Critical

<sup>a)</sup>Address all correspondence to this author.  
e-mail: grana@szfki.hu

This paper was selected as the Outstanding Meeting Paper for the 2004 MRS Fall Meeting Symposium JJ Proceedings, Vol. 859E.  
DOI: 10.1557/JMR.2006.0011

fluctuations forming on reasonable experimental time scales contain typically tens to several hundred molecules.<sup>3–6</sup> This situation, combined with the fact that the crystal–liquid interface extends several molecular layers,<sup>7</sup> suggests that critical fluctuations are fundamentally interfacial in nature. Essentially, when the interface dimensions approach those of the critical fluctuation, the consequences of interfacial diffuseness must be considered. The droplet model of classical nucleation theory, which employs a sharp interface separating a liquid from a crystal with bulk properties, is therefore an extreme idealization of such diffuse interfaces, as has been demonstrated by recent atomistic simulations.<sup>6</sup>

Field theoretical models that predict a diffuse interface, offer a natural way to handle such difficulties,<sup>8</sup> and have proved successful in addressing nucleation problems, including nucleation of metastable phases.<sup>9,10</sup>

The polycrystalline morphologies observed in Nature, the laboratory, and technological applications can be divided into two main classes: (i) those formed by the impingement of independently nucleated single crystals (formed by primary nucleation) and (ii) the polycrystalline growth forms that consist of an increasing number of crystalline grains nucleating continuously at the perimeter of the particle (often called secondary nucleation). Examples of such morphologies<sup>11–16</sup> are shown in Fig. 1. The complexity of polycrystalline freezing is especially obvious in the case of thin (a few tens of nanometers) polymer layers, which show an enormous richness in their crystallization morphologies [see e.g., Figs. 1(c),

1(e) and 1(f)]. These quasi two-dimensional structures give important clues to the mechanisms that govern the formation of polycrystalline patterns.

In the past decade, the phase field theory became the method of choice when describing complex solidification morphologies, including dendrites, eutectic, and peritectic structures.<sup>17,18</sup> The fact that similar polycrystalline patterns are observed in systems of very different nature (metals, polymers, biopolymers) suggests that a minimal model based on coarse-grained fields that neglects the details of molecular interactions might be appropriate. Such a mesoscopic model may have advantages relative to previous macroscopic<sup>19,20</sup> and microscopic models.<sup>21,22</sup> Although this field-theoretic approach disregards most of the molecular scale details of solidification, some features such as crystal symmetries can be incorporated via the anisotropies of the model parameters. The rationale for developing such coarse-grained models is the current inability of fully molecular models<sup>21,22</sup> to address the formation of such large scale morphologies. It is anticipated that these coarse-grained models will contribute to a better understanding of some of the dominant factors required for the formation of polycrystals.

In this paper, we briefly review recent advances made in the application of the phase field simulations for describing both homogeneous and heterogeneous crystal nucleation, as well as polycrystalline growth in complex liquids. The interested reader may find further details in Refs. 23–29.

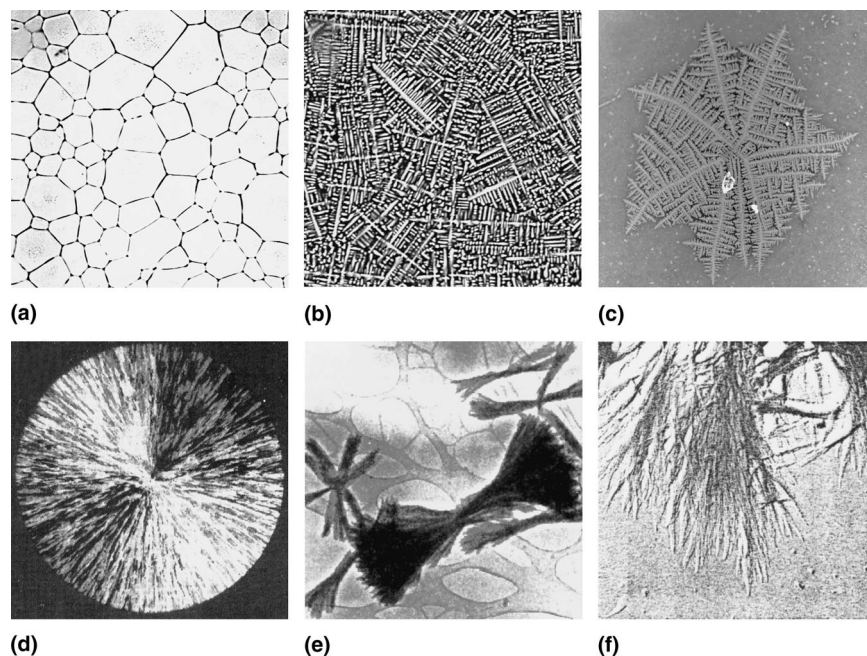


FIG. 1. Polycrystalline microstructures: (a) polycrystalline morphology formed by impinging single crystals,<sup>11</sup> (b) polycrystalline morphology formed by impinging dendrites in the oxide glass  $(\text{ZnO})_{61.4}(\text{B}_2\text{O}_3)_{38.6}(\text{ZnO}_2)_{28}$ ,<sup>12</sup> (c) “dizzy” dendrite formed in clay filled polymethyl methacrylate-polyethylene oxide thin film,<sup>13</sup> (d) spherulite formed in pure Se,<sup>14</sup> (e) crystal sheaves in pyromellitic dianhydride-oxydianilin poly(imid) layer,<sup>15</sup> and (f) arboresque growth form in polyglycine.<sup>16</sup>

## II. PHASE FIELD MODEL FOR POLYCRYSTALLINE SOLIDIFICATION

First, we outline the general features of our model for polycrystalline freezing,<sup>23</sup> which builds on an earlier model of crystallization with vector-valued phase field.<sup>30</sup> The local thermodynamic state of matter is characterized by the phase field  $\phi$  that monitors the liquid–solid phase transition. This order parameter describes the extent of structural change during freezing and melting. The other basic field variables are the chemical composition  $c$  and the normalized orientation field  $\theta$ , where  $\theta$  specifies the orientation of crystal planes in the laboratory frame. While a single orientation field is satisfactory in two dimensions, generalization of the model for three dimensions require minimum three orientation fields.<sup>31,32</sup> Herein, we concentrate mainly on two-dimensional (2D) problems, which have been studied as a reasonable approximation in previous experimental studies.

The free energy  $F$  consists of various contributions that will be discussed below:

$$F = \int d^3r \left\{ \begin{array}{l} \frac{\epsilon_\phi^2 T}{2} s^2 (\vartheta - \theta) |\nabla \phi|^2 + w(c) T g(\phi) \\ + [1 - p(\phi)] [f_s(c, T) + f_{\text{ori}}(|\nabla \theta|)] \\ + p(\phi) f_L(c, T) \end{array} \right\}, \quad (1)$$

where

$$\begin{aligned} \epsilon_\phi^2 &= \frac{6\sqrt{2}\gamma_{A,B}\delta_{A,B}}{T_{A,B}}, \\ w(c) &= (1 - c)w_A + cw_B, \\ w_{A,B} &= \frac{12\gamma_{A,B}}{\sqrt{2}\delta_{A,B}T_{A,B}}, \\ g(\phi) &= \frac{1}{4}\phi^2(1 - \phi)^2, \\ p(\phi) &= \phi^3(10 - 15\phi + 6\phi^2), \\ f_{\text{ori}} &= HT|\nabla \theta|, \\ s(\vartheta - \theta) &= 1 + s_0 \cos(k\vartheta - 2\pi\theta), \\ \vartheta &= \arctan[(\nabla \phi)_y / (\nabla \phi)_x]. \end{aligned}$$

Here  $\epsilon_\phi$  is the coefficient of the square-gradient term for the field  $\phi$ ,  $w_i$  is the free energy scale for the  $i$ th pure component ( $i = A, B$ ),  $f_s$  and  $f_L$  are the free energy densities of the bulk solid and liquid phases, while  $f_{\text{ori}}$  is the orientational contribution to the free energy density.  $\gamma_i$ ,  $\delta_i$ ,  $T_i$  are the interface free energy, interface thickness, and melting point for the  $i$ th pure component.  $s$ ,  $g$ , and  $p$  are the anisotropy function, quartic double-well function,

and interpolation function, respectively.  $\vartheta$  is the inclination of the normal vector of the interface in the laboratory frame,  $s_0$  is the amplitude of the anisotropy of the interface free energy, while  $k$  is the symmetry index ( $k = 6$  for 6-fold symmetry).  $H$  determines the free energy of the low angle grain boundaries. Time evolution is governed by relaxational dynamics, and Langevin noise terms are added to model thermal fluctuations.

The time scales for the three fields are determined by the appropriate mobilities appearing in the equations of motion, and  $M_\phi$ ,  $M_c$ , and  $M_\theta$  are the mobilities associated with coarse-grained equation of motion, which in turn are related to their microscopic counterparts. The mobility  $M_c$  is directly proportional to the classic interdiffusion coefficient for a binary mixture. The mobility  $M_\phi$  dictates the rate of crystallization, while  $M_\theta$  controls the rate at which regions reorient. The equations of motion are described in detail elsewhere.<sup>23,27</sup>

The orientation contribution to the free energy  $f_{\text{ori}}$  represents the excess free energy due to inhomogeneities in crystal orientation in space, in particular, the misorientation due to a grain boundary, represented by spatial variation of the orientation field  $\theta$ , whose local value specifies the orientation angle that, in turn, sets the tilt of the crystal planes in the laboratory frame. The angular dependence of the interfacial free energy and/or the kinetic coefficient needed for addressing anisotropic growth is measured relative to this orientation. Due to the non-analytic nature of the orientational free energy density  $f_{\text{ori}}$ , the equation of motion specifies a singular diffusivity problem and requires special care when handled numerically.<sup>33</sup> Various modifications of this approach have been applied for describing competing growth of anisotropic particles, including dendritic solidification in an undercooled liquid.<sup>23,30</sup> Applications to grain boundary problems, including grain boundary wetting and grain coarsening in polycrystalline matter via grain boundary migration and rotation, have been described by us in our recent work.<sup>34</sup>

Modeling of nucleation of grains at the solidification front requires a further important element. Gránásy et al.<sup>23</sup> extended the orientation field  $\theta$  into the liquid phase and allowed it to fluctuate in time and space. Assigning a local crystal orientation to liquid regions, even a fluctuating one, may seem artificial at first sight. However, due to geometrical and/or chemical constraints, short-range order exists even in simple liquids. Microscopically, we can rotate the crystalline first-neighbor shell so that it aligns optimally with the local liquid structure, and, in this way, one may assign a local orientation to every atom in the liquid. The orientation obtained in this manner indeed fluctuates in time and space. The correlation of the atomic positions/angles shows how appropriate this approximation is. (In the phase field model, the fluctuating orientation field and the phase field play

these roles.) Approaching the solid from the liquid, the orientation becomes more definite (the amplitude of the orientational fluctuations decreases) and matches to that of the solid while the correlation between the local liquid structure and the crystal structure improves. In this model, the orientation field and the phase field are strongly coupled to recover this behavior.

The phase field theory can be used for calculating the height of the nucleation barrier to initiate crystallization.<sup>23,24,27,35</sup> Because the equilibrium is unstable, the critical fluctuation (the nucleus) can be found as an extremum of the free energy functional, subject to conservation constraints when the phase field is coupled to conserved fields such as solute concentration or energy. To mathematically impose such constraints, one adds the volume integral over the conserved field times a Lagrange multiplier to the free energy. The field distributions that extremize the free energy obey the appropriate Euler–Lagrange equations, which, in the phase field theory, take the form

$$\frac{\delta F}{\delta \psi} = \frac{\partial I}{\partial \psi} - \nabla \cdot \frac{\partial I}{\partial \nabla \psi} = 0 \quad , \quad (2)$$

where  $\delta F/\delta \psi$  stands for the first functional derivative of the free energy with respect to the field  $\psi$ , while  $I$  is the total free energy density (the gradient terms are included). Here  $\psi$  stands for all the fields used in theory. The Euler–Lagrange equations are solved assuming that unperturbed liquid exists in the far-field, while, for symmetry reasons, zero field gradients exist at the center of the fluctuations. The same solutions can also be obtained as the non-trivial time-independent solution of the governing equations for field evolution. Having determined the solutions, the work of forming a nucleus (height of the nucleation barrier) can be obtained by inserting the solution to Eq. (2) into the free energy functional.

In large-scale phase field simulations, one is often compelled by computational limitations to use an unphysically broad interface. However, in the case of nucleation, where the interface thickness and the size of nuclei are comparable, one can work with the physical interface thickness. In a few cases, all parameters of the phase field theory can be fixed, and the calculations can be performed without adjustable parameters. For example, in the one-component limit of the standard binary phase field theory, the free energy functional contains only two parameters, the coefficient of the square-gradient term for phase field and the free energy scale (height of the central hill between the double well in the local free energy density). If the thickness and the free energy of a crystal–liquid interface are known for the equilibrium crystal–liquid interface, all model parameters can be fixed, and the properties of the critical fluctuation, including the height of the nucleation barrier,

can be predicted without adjustable parameters. Such information is available from atomistic simulations/experiments for only a few model fluids (Lennard–Jones fluids and water). We have found a good quantitative agreement with the magnitude of the nucleation barriers deduced from atomistic simulations for the Lennard–Jones system and from experiments on ice nucleation in undercooled water.<sup>23</sup> Similar results have been obtained for the hard-sphere system using a phase field model that relies on a structural order parameter coupled to the density field.<sup>24</sup> Again, the model parameters have been fixed via the interface thickness and interfacial free energy from atomistic simulations, so the calculations were performed without adjustable parameters. Herein we present an extended test of theory for the hard-sphere system.

The phase-field theory can also be used to simulate the nucleation process itself. The proper statistical mechanical treatment of the nucleation process requires the introduction of uncorrelated Langevin-noise terms into the governing equations with amplitudes that are determined by the fluctuation-dissipation theorem.<sup>23,36,37</sup> Such an approach has been used for describing homogeneous nucleation in a single-component<sup>37</sup> and binary alloy systems<sup>23</sup> and during eutectic solidification in a binary model.<sup>36</sup>

Solidification in the presence of walls is of great practical importance. In casting, solidification usually starts by heterogeneous crystal nucleation on the walls of the mold. With the exception of extremely pure samples, even nucleation in the bulk liquid happens mostly via a heterogeneous mechanism (on the surface of suspended foreign particles). Particulate additives are widely used as grain refiners to reduce grain size by enhancing the nucleation rate. Heterogeneous nucleation is probably the least understood stage of solidification since the molecular scales of this self-organization normally precludes direct observation of the process.

Although the phase field method has been used to address problems that incorporate heterogeneous nucleation, this type of nucleation is usually mimicked by introducing supercritical particles into the simulation window (supercritical particles exceed the minimum radius needed to ensure the particles growth). Recently, steps have been made toward a physical modeling of heterogeneous nucleation within the phase field theory. Castro<sup>37</sup> introduced walls (boundaries) into a single order parameter theory by assuming a no-flux boundary condition at the interface ( $\mathbf{n} \cdot \nabla \phi = 0$ , where  $\mathbf{n}$  is the normal vector of the wall), which results in a contact angle of  $90^\circ$  at the wall–solid–liquid triple junction. Langevin noise is then introduced to model nucleation. In this work, we generalize this approach to the nucleation of crystallites with different crystallographic orientation in a binary system. Prescribing  $(\mathbf{n} \cdot \nabla \phi) = 0$  and  $(\mathbf{n} \cdot \nabla c) = 0$  at the wall perimeter, we introduced chemically inert surfaces,

and performed simulations to address heterogeneous volume nucleation on foreign particles, on rough surfaces, and in confined space (porous materials and regular channels).<sup>27</sup>

### III. RESULTS AND DISCUSSION

#### A. Homogeneous nucleation

Recent developments in atomistic modeling of small crystalline clusters in the hard-sphere system allow for an extension of the quantitative analysis described in Ref. 24. Cacciuto et al.<sup>38</sup> evaluated the free energy of clusters in the hard-sphere liquid of equilibrium density as function of size that allowed the determination of the size dependence of the solid-liquid interface free energy. The results extrapolate to  $\gamma_{R \rightarrow \infty} = 0.616(3)kT/\sigma^2$ , the cluster average of the interfacial free energy for infinite size ( $\sigma$  is diameter of the hard spheres). This value agrees well with results from molecular dynamics simulations [e.g., with  $\gamma_{av}/(kT/\sigma^2) = 0.612 \pm 0.02$  for the average of the values for the (111), (110), and (100) directions by Davidchack and Laird<sup>7</sup>; and with  $\gamma_{av}/(kT/\sigma^2) = 0.63 \pm 0.02$  by Mu et al.<sup>39</sup>]. This allows us to fix the coefficient of the square-gradient term with a higher accuracy than in previous work, since it was previously uncertain how far the cluster (or orientational) average of the interfacial free energy falls from the average for the (111), (110), and (100) directions. A further refinement of the theory is that the density dependence of the coefficient of the square-gradient term,  $\epsilon^2 \propto d^2C(k)/dk^2$ , and of the free energy scale,  $w \propto 1/S(k)$ , are taken into consideration,

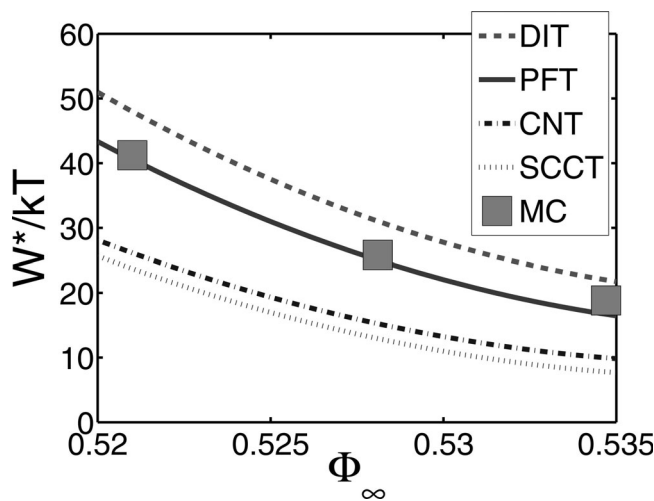
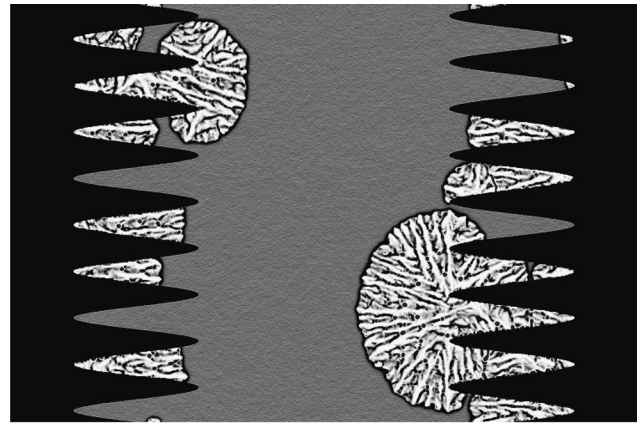
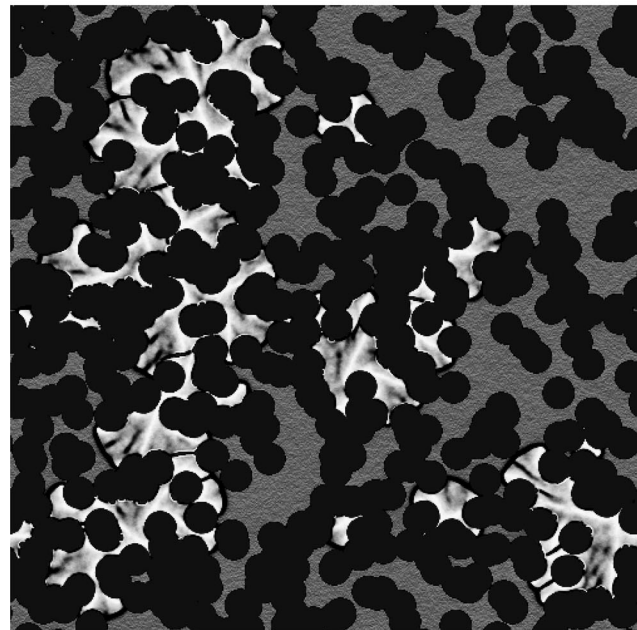


FIG. 2. Height of the nucleation barrier versus the initial density of the hard-sphere liquid as predicted by the phase field theory (PFT),<sup>40</sup> sharp interface droplet model of the classical nucleation theory (CNT), self-consistent classical theory (SCCT),<sup>41</sup> and phenomenological diffuse interface theory (DIT).<sup>42</sup> These calculations contain no adjustable parameters. For comparison, the height of the nucleation barrier from Monte Carlo simulations is also included in the figure.<sup>6</sup>



(a)

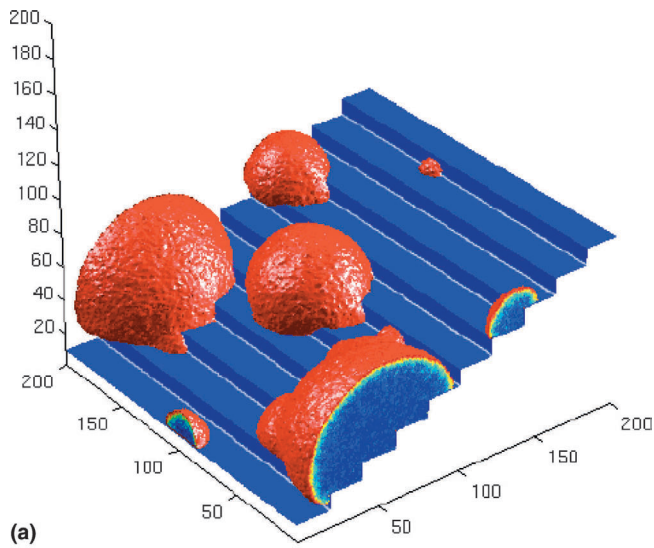


(b)

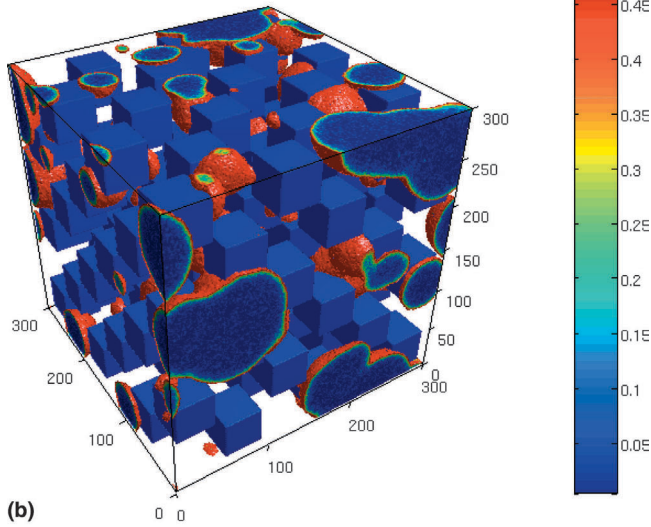


(c)

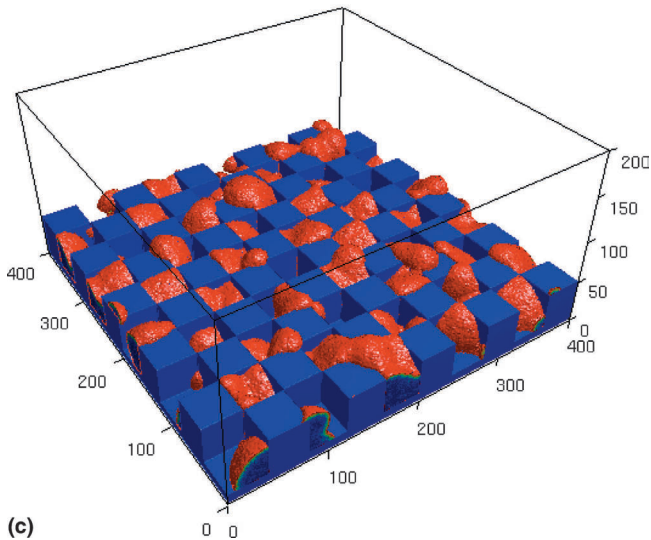
FIG. 3. Solidification in the presence of walls/particles as predicted by the phase field theory. (a) Heterogeneous nucleation on rough surfaces (walls are gray). (b) Heterogeneous nucleation and crystallization in porous matter (blue: particles of porous matter; bright yellow: crystal, khaki: liquid). Note that nucleation happens in the notches between particles of the porous matter. (c) Dendritic solidification in a 2D orientation selector (pigtail) mimicking the casting of single crystal components. Composition field is shown (blue: solidus; yellow: liquid; grey: mold).



(a)

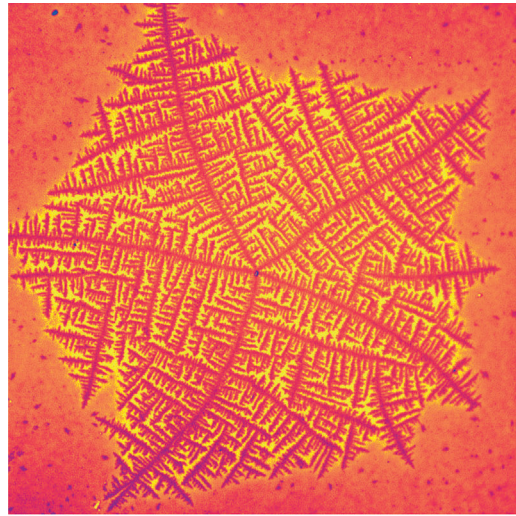


(b)



(c)

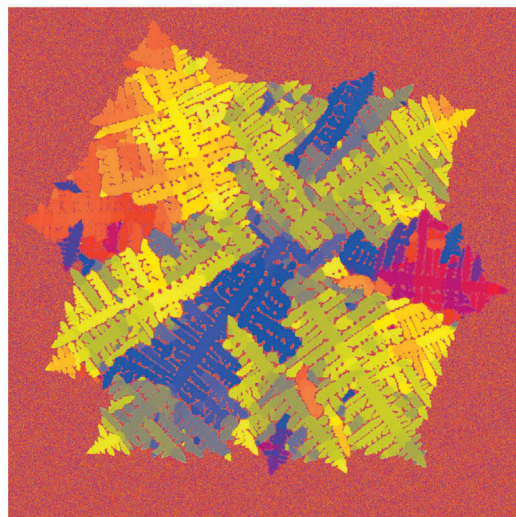
FIG. 4. Heterogeneous nucleation in 3D: (a) on stairs, (b) in porous matter represented by cubes (foreign particles) positioned on a bcc lattice, and (c) on a checkerboard-modulated surface.



(a)



(b)



(c)

FIG. 5. “Dizzy” dendrites in experiment (a) and phase field simulations [(b) composition; (c) orientation].<sup>25</sup>

where  $C(k)$  is the direct correlation function of the liquid which is related to the structure factor of the liquid via  $S(k) = 1/[1 - C(k)]$ . The parameter-free predictions of the phase field theory (PFT) and the exact Monte Carlo (MC) results are compared in Fig. 2.<sup>40</sup> The agreement between theory and MC simulations is highly encouraging; the agreement is considerably better than the (parameter-free) predictions of the classical nucleation theory and the self-consistent classical theory of Girshick and Chiu,<sup>41</sup> and the fit also improves upon the parameter-free prediction by the phenomenological diffuse interface theory of Gránásy.<sup>42</sup> The uncertainty of the input data (interfacial free energy, equations of state, etc.) does not influence this result perceptibly.<sup>40</sup>

This confirmation of our previous findings<sup>24</sup> suggests that the phase field theory is able to predict the height of the nucleation barrier quantitatively, when the physical interface thickness is used as input information. This success, together with the parameter-free prediction of the dendritic growth rate,<sup>18</sup> suggests that a multi-scale approach to the phase field theory with model parameters deduced from atomistic simulations is capable of quantitative predictions for both crystal nucleation and growth, at least for simple liquids.

## B. Heterogeneous nucleation

We have also recently addressed heterogeneous crystal nucleation in the framework of the PFT.<sup>27</sup> A few results, which illustrate that various complex phenomena can be addressed this way are shown in Fig. 3. We show noise-induced nucleation on particles and rough surfaces, particle engulfment, solidification in porous medium, and in a rectangular channel (orientation selector), in both two and three dimensions. In the three-dimensional (3D) calculations, a simpler model is used, which does not account for the differences in the crystallographic orientation.<sup>27</sup> Heterogeneous noise-induced nucleation has been investigated in 3D for various geometries including a

stairlike surface, porous medium (represented by cubes placed on a bcc lattice), and 3D checkerboard-like modulated surface (Fig. 4). Such studies may contribute to a better understanding of processes that can be used in micro/nano-patterning.

## C. Polycrystalline growth

A spectacular class of structures appears in thin polymer blend films if foreign (clay) particles are introduced.<sup>13</sup> A disordered dendritic structure termed a “dizzy” dendrite (Fig. 5) forms by the engulfment of the clay particles into the crystal, inducing the formation of new grains. This phenomenon is driven by the impetus to reduce the crystallographic misfit along the perimeter of clay particles by creating grain boundaries within the polymer crystal. This process changes the crystal orientation at the dendrite tip, changing thus the tip trajectory (tip deflection). To describe this phenomenon, Gránásy et al.<sup>25</sup> incorporated a simple model of foreign crystalline particles into the phase field theory: they are represented by orientation pinning centers—small areas of random, but fixed orientation—which are assumed to be of a foreign material, and not the solid  $\phi = 0$  phase. This picture economically describes morphological changes deriving from particle-dendrite interactions. Using an appropriate density of pinning centers, comparable to the density of clay particles, a striking similarity is obtained between experiment and simulation (Fig. 5). This description extends to such fine details as curling of the main arms and the appearance of extra arms. The disorder in the dendritic morphology reflects the underlying polycrystalline structure that emerges as dendrite tips deflect on foreign particles.

The mechanism described above is certainly not a general explanation for all polycrystalline growth since spherulites have been observed to grow in liquids without particulates or detectable molecular impurities. The question is how this can be understood. A clue to this

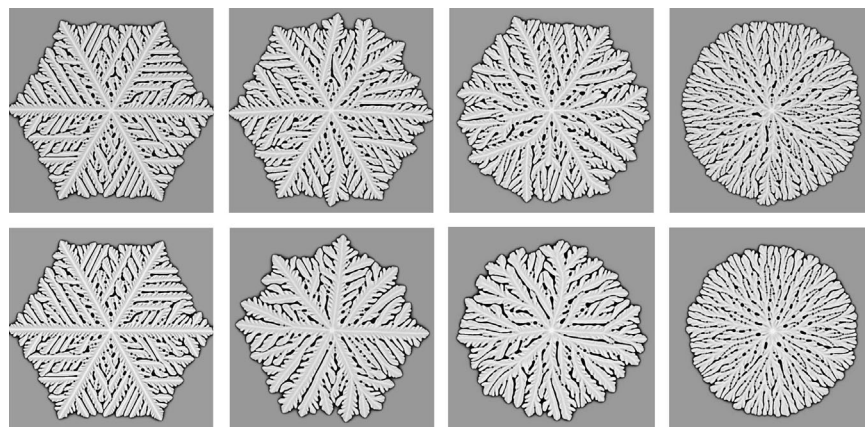


FIG. 6. Here the dendrite to seaweed transition is induced either by particulate additives (upper row, number of particulates increases from left to right), or by reducing the orientational mobility (lower row: mobility decreases from left to right).<sup>26,27</sup>

phenomenon can be found in the observations of Magill,<sup>43</sup> who noted that spherulites only seem to appear in highly undercooled pure fluids of sufficiently large viscosity. Based on the observations summarized by Magill, we hypothesize that the decoupling of the translational and rotational diffusion coefficient is responsible for the propensity for polycrystalline growth in highly undercooled liquids. Specifically, a reduced  $D_{\text{rot}}$  should make it difficult for newly forming crystal regions to reorient with the parent crystal to lower its free energy at the growth front that is advancing with a velocity scaling with the translational diffusion coefficient. Thus, epitaxy cannot keep pace with solidification, and consequently the orientational order that freezes in is incomplete. We

term this phenomenon growth front nucleation (GFN). This situation can be captured within the phase field theory by reducing the orientational mobility while keeping the phase field mobility constant as discussed in detail by Gránásy et al.<sup>26</sup>

We recently performed a systematic study<sup>26,27</sup> of polycrystalline morphologies forming via particulate induced GFN and low orientation mobility induced GFN, and found that the two mechanisms lead to strikingly similar morphologies and grain structures (see Fig. 6). These results demonstrate a duality between the morphologies evolving due to the effects of static heterogeneities (foreign particles) and dynamic heterogeneities (quenched-in orientational defects). It is thus natural that polycrystalline

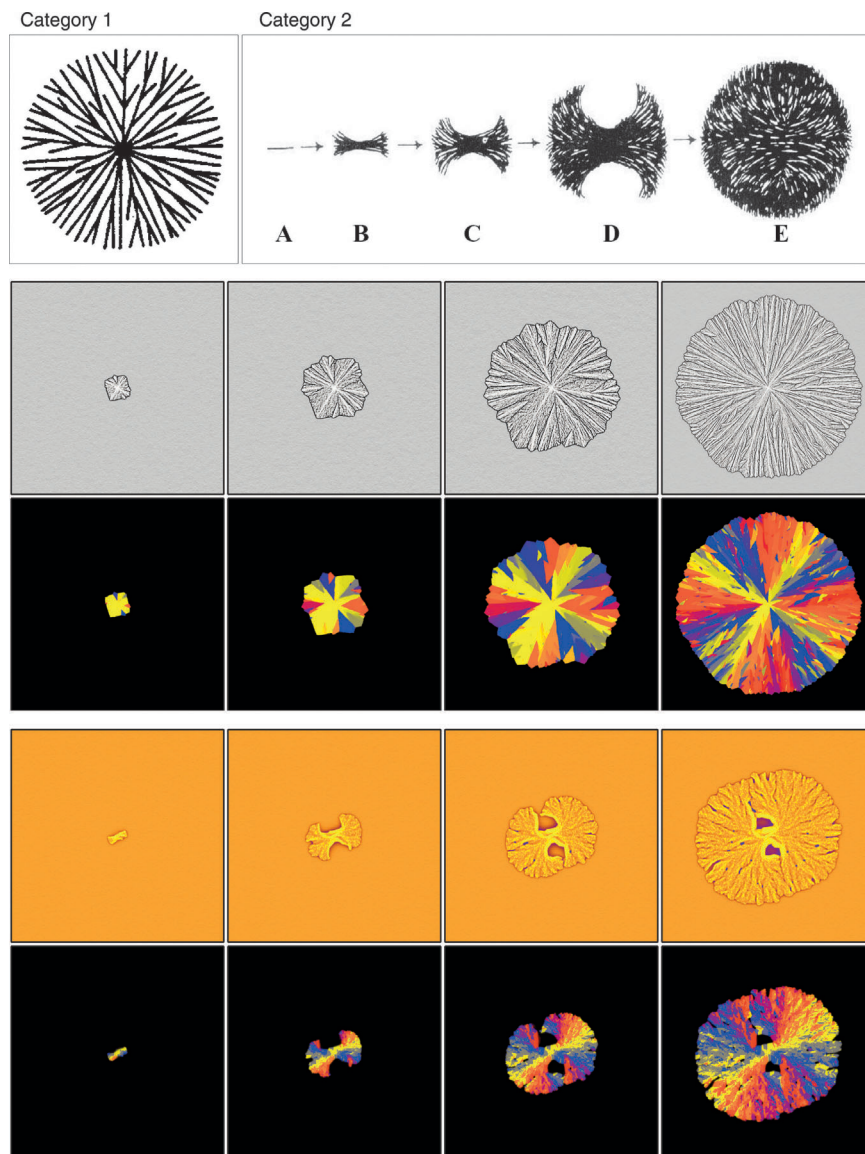


FIG. 7. Formation of polycrystalline spherulites. Upper block: Concepts for the formation of Category 1 and 2 spherulites.<sup>44</sup> Central block: Formation of a Category 1 spherulite in the phase field theory. Bottom block: Formation of a Category 2 spherulite in the phase field theory. In the central and lower blocks images in the upper row show the composition field, while in the lower row the respective orientation field is displayed. (In the orientation maps different colors correspond to different crystallographic orientations.)

growth is prevalent in fluids crystallized in heterogeneous materials such as gels, as well as in highly supercooled liquids such as those commonly found during the processing of polymeric materials.

#### D. Formation of spherulites

Experimental studies performed over the last century indicate that there are two main categories of growth forms commonly termed spherulites.<sup>43</sup> Category 1 spherulites grow radially from the nucleation site, branching intermittently to maintain a space filling character (Fig. 7). In contrast, Category 2 spherulites grow initially as thread-like fibers subsequently forming new and new branches at the growth front (Fig. 7). This branching of the crystallization pattern ultimately leads to a crystal “sheaf” structure that increasingly splays out during growth. At still longer times, these sheaves develop two “eyes” (uncrystallized regions) on each side of the primary nucleation site. Ultimately, this type of spherulite settles down into a spherical growth pattern, with eye structures apparent in its core region. In some materials, both categories of spherulite occur in the same material under the same nominal thermodynamic conditions.

One of the popular ideas used to explain the formation of spherulites envisions that these structures arise from the regular branching of crystalline filaments having a well-defined branching angle (see e.g., Refs. 43–45). While the details of such a mechanism necessarily differ on the molecular scale for the many systems that display spherulitic solidification, we hope to capture the general features of this process within a phase field model that accounts for this branching process. To incorporate branching with a fixed orientational misfit, we included a new form of the orientational free energy. Here the orientational free energy has a second (local) minimum as a function of misorientation angle  $\xi_0|\nabla\theta|$ , where  $\xi_0$  is the correlation length of the orientation field. Thus, during orientational ordering at the solid–liquid interface, a second (metastable) free energy can be selected by the system, corresponding to a particular preferred grain misorientation. Accordingly, the cells that have a larger misorientation, than the first (local) maximum of the  $f_{\text{ori}}$  versus  $\xi_0|\nabla\theta|$  relationship, may relax toward the local minimum, unless the orientational noise prevents them from settling into this minimum.

Category 1 spherulites (described above) have been seen to form from transient single-crystal nuclei.<sup>46</sup> Our model captures the gradual transition from square-shaped single crystals to circular shape under isothermal conditions. As seen in simulation, square-shaped single crystals nucleate after an initial incubation period. After exceeding a critical size (that depends on the ratio  $\chi$  of the rotational and translational diffusion coefficients), the growing crystal cannot establish the same crystallographic orientation along its perimeter. Thus, new grains

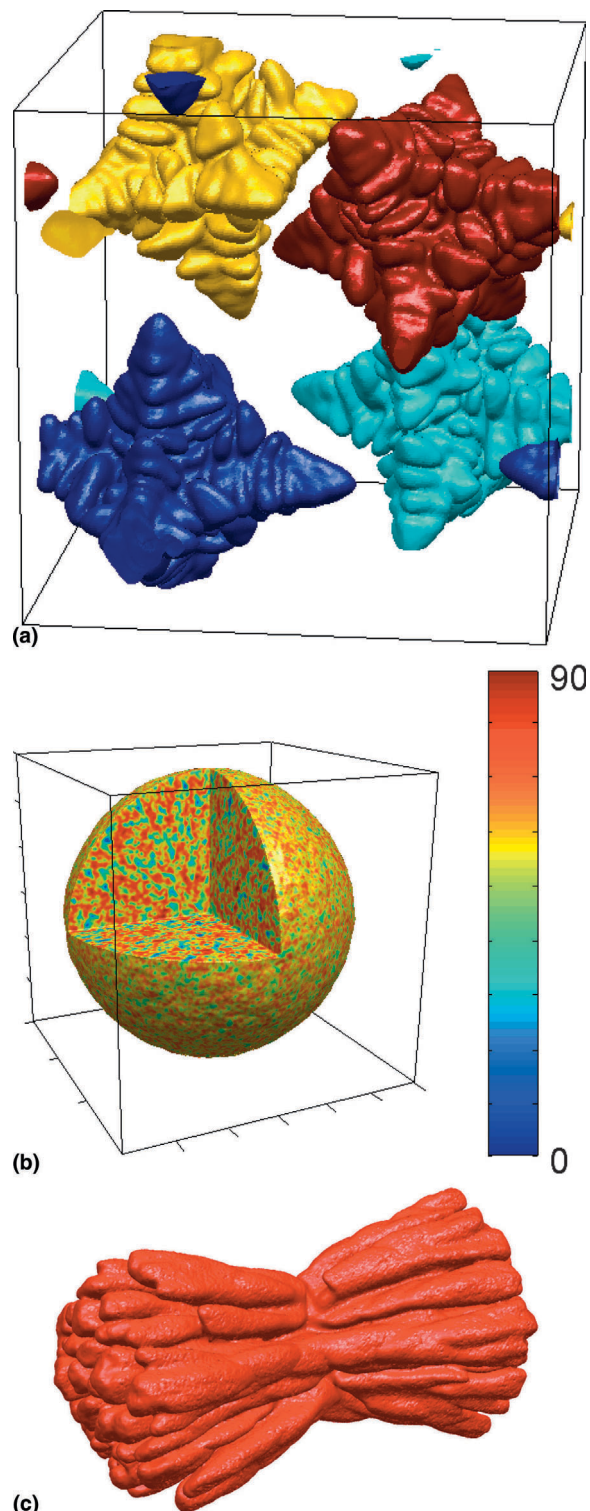


FIG. 8. Polycrystalline freezing in 3D as predicted by the phase field theory.<sup>47</sup> (a) Growth of four randomly oriented dendrites assuming cubic crystal symmetries ( $400 \times 400 \times 400$  grid). (b) Polycrystalline spherulite formed by trapping of orientational disorder calculated with triclinic crystal symmetry ( $300 \times 300 \times 300$  grid). The growth front is colored according to the angular difference between the  $z$ -axes of the local and laboratory frames (see color bar). (c) A crystal sheaf formed by branching of a needle crystal simulated with triclinic crystal symmetry ( $250 \times 250 \times 500$  grid). The  $\phi = 0.5$  surface is shown.

form by secondary nucleation as described in the introduction. This process gradually establishes a circular perimeter for mature growth forms (Fig. 7). In agreement with experiment, analyses of simulations for Category 1 spherulites indicate a constant radial growth rate.<sup>28,29</sup>

Many studies of the early stages of spherulite growth, especially in polymers, indicate that these structures initially grow as slender threadlike fibers.<sup>43–45</sup> These structures successively branch to form space-filling patterns. A large kinetic anisotropy of 2-fold symmetry is assumed, as is appropriate for polymeric systems that have a propensity to form crystalline filaments.<sup>28,29</sup> We include a preferred misorientation angle of 30°. Ideally, in a system where filament branching happens with a 30° misfit, the polycrystalline growth form may consist of only grains that have six well-defined orientations (including the one that nucleated), and which differ in orientation by multiples of 30°. With increasing driving force, the branching frequency increases, and more space filling patterns emerge, while the average grain size decreases. This leads to a continuous morphological transition that links the needle-crystals forming at low supersaturation, to crystal sheaves (“axialites”), and to Category 2 spherulites (with “eyes” on the two sides of the nucleus) under far from equilibrium growth conditions.<sup>28,29</sup>

The time evolution of a Category 2 spherulite is shown in Fig. 7. First, fibrils form and then secondary fibrils nucleate at the growth front to form crystal “sheaves.” The diverging ends of these sheaves subsequently fan out with time to form eyes, and finally a roughly spherical growth form emerges.<sup>28,29</sup> This progression of spherulitic growth is nearly universal in polymeric materials.<sup>43–45</sup>

A recent development is that the polycrystalline model used in the simulations shown above has been extended to three dimensions.<sup>33,34</sup> We present illustrative calculations for various polycrystalline growth modes in Fig. 8. This figure shows snapshots of the growth of randomly oriented dendritic particles of cubic crystal symmetries and the formation of a polycrystalline spherulite and a crystal sheaf.<sup>47</sup>

#### IV. CONCLUDING REMARKS

We have reviewed recent advances in phase field modeling of polycrystalline structures. It has been shown that phase field models relying on orientation fields offer a general approach to polycrystalline solidification and can be used to address various processes relevant to polycrystalline freezing such as homogeneous and heterogeneous modes of primary and secondary nucleation. One of the major challenges we faced was the description of foreign particles. In this, we relied on two simple models: (i) the orientation pinning centers, and

(ii) particles defined by walls of 90° contact angle. While these simplistic approaches are indeed successful in capturing dominant features of particle-induced disorder in polycrystalline growth, a full model of foreign particles that takes their composition and crystallographic properties into account remains to be developed.

Finally, we find it remarkable that a simple coarse-grained field theory consisting of only a few model parameters is able to address the formation of a broad variety of polycrystalline morphologies seen in nature and laboratory, including disordered dendrites, spherulites, fractal-like aggregates, and many more.

#### ACKNOWLEDGMENTS

The authors thank V. Ferreiro for the images on transformation in polymer thin films, V. Fleury for the picture on the electrodeposited patterns, and G. Faivre for the image on the Se spherulite. This work was supported by contracts OTKA-T-037323, ESA PECS Contract No. 98005, and by the EU FP6 Integrated Project IMPRESS under Contract No. NMP3-CT-2004-500635, and forms part of the ESA MAP Project Nos. AO-99-101 and AO-99-114. Tomás Pusztai acknowledges support by the Bolyai János Scholarship of the Hungarian Academy of Sciences.

#### REFERENCES

1. L.-W. Jin, K.A. Claborn, M. Kurimoto, M.A. Geday, I. Maezawa, F. Sohraby, M. Estrada, W. Kaminsky, and B. Kahr: Imaging linear birefringence and dichroism in cerebral amyloid pathologies. *Proc. Natl. Acad. Sci. U S A* **100**, 15297 (2003).
2. *Proc. Royal Soc. Discussion Meeting on Nucleation Control*, edited by G.W. Greenwood, A.L. Greer, D.M. Herlach, and K.F. Kelton, *Philos. Trans.* **361** (2003).
3. W.C. Swope and H.C. Andersen: 10<sup>6</sup>—particle molecular-dynamics study of homogeneous nucleation of crystals in a supercooled atomic liquid. *Phys. Rev. B* **41**, 7042 (1990).
4. P.R. ten Wolde and D. Frenkel: Homogeneous nucleation and the Ostwald step rule. *Phys. Chem. Chem. Phys.* **1**, 2191 (1999).
5. P.R. ten Wolde, M.J. Ruiz-Montero, and D. Frenkel: Numerical evidence for bcc ordering at the surface of critical fcc nucleus. *Phys. Rev. Lett.* **75**, 2714 (1995).
6. S. Auer and D. Frenkel: Prediction of absolute crystal-nucleation rate in hard-sphere colloids. *Nature* **409**, 1020 (2001).
7. R.L. Davidchack and B.B. Laird: Direct calculation of the hard-sphere crystal/melt interfacial free energy. *J. Chem. Phys.* **108**, 9452 (1998).
8. D.W. Oxtoby: Density-functional methods in the statistical mechanics of materials. *Annu. Rev. Mater. Res.* **32**, 39 (2002).
9. Y.C. Shen and D.W. Oxtoby: Bcc symmetry in the crystal-melt interface of Lennard-Jones fluids examined through density-functional theory. *Phys. Rev. Lett.* **77**, 3585 (1996).
10. L. Gránásy and D.W. Oxtoby: Cahn–Hilliard theory with triple parabolic free energy. II. Nucleation and growth in the presence of a metastable crystalline phase. *J. Chem. Phys.* **112**, 2410 (2000).
11. K. Lee and W. Losert: Private communication (2004).
12. B.D. Nobel and P.F. James: Private communication (2003).
13. V. Ferreiro, J.F. Douglas, J.A. Warren, and A. Karim: Growth

- pulsation in symmetric dendritic crystallization in thin polymer blend films. *Phys. Rev. E* **65**, 051606 (2002).
14. G. Ryshchenkow and G. Faivre: Bulk crystallization of liquid selenium—Primary nucleation, growth-kinetics and modes of crystallization. *J. Cryst. Growth* **87**, 221 (1988).
  15. M. Ojeda and D.C. Martin: High-resolution microscopy of PMDA-ODA poly(imide) single crystals. *Macromol.* **26**, 6557 (1993).
  16. F.J. Padden and H.D. Keith: Crystalline morphology of synthetic polypeptides. *J. Appl. Phys.* **36**, 2987 (1965).
  17. W.J. Boettinger, J.A. Warren, C. Beckermann, and A. Karma: Phase-field simulation of solidification. *Ann. Rev. Mater. Res.* **32**, 163 (2002).
  18. J.J. Hoyt, M. Asta, and A. Karma: Atomistic and continuum modeling of dendritic solidification. *Mater. Sci. Eng. Rep.* **R41**, 121 (2003).
  19. H.D. Keith and F.J. Padden, Jr.: A phenomenological theory of spherulitic crystallization. *J. Appl. Phys.* **34**, 2409 (1963).
  20. N. Goldenfeld: Theory of spherulitic solidification. *J. Cryst. Growth* **84**, 601 (1987).
  21. K. Nagarajan and A.S. Myerson: Molecular dynamics of nucleation and crystallization of polymers. *Cryst. Growth Design* **1**, 131 (2005).
  22. T. Yamamoto: Molecular dynamics modeling of polymer crystallization from the melt. *Polymer* **45**, 1357 (2004).
  23. L. Gránásy, T. Börzsönyi, and T. Pusztai: Nucleation and bulk crystallization in binary phase field theory. *Phys. Rev. Lett.* **88**, 206105 (2002).
  24. L. Gránásy, T. Pusztai, G. Tóth, Z. Jurek, M. Conti, and B. Kvamme: Phase field theory of crystal nucleation in hard-sphere liquid. *J. Chem. Phys.* **119**, 10376 (2003).
  25. L. Gránásy, T. Pusztai, J.A. Warren, T. Börzsönyi, J.F. Douglas, and V. Ferreiro: Growth of ‘dizzy dendrites’ in a random field of foreign particles. *Nat. Mater.* **2**, 92 (2003).
  26. L. Gránásy, T. Pusztai, T. Börzsönyi, J.A. Warren, and J.F. Douglas: A general mechanism of polycrystalline growth. *Nat. Mater.* **3**, 645 (2004).
  27. L. Gránásy, T. Pusztai, and J.A. Warren: Modelling polycrystalline solidification using phase field theory. *J. Phys.: Condens. Matter* **16**, R1205 (2004).
  28. L. Gránásy, T. Pusztai, G. Tegze, J.A. Warren, and J.F. Douglas: On the growth and form of spherulites. *Phys. Rev. E* **72**, 011605 (2005).
  29. L. Gránásy, T. Pusztai, G. Tegze, J.A. Warren, and J.F. Douglas: Polycrystalline patterns in far-from-equilibrium freezing: A phase field study. *Philos. Mag. A* (in press).
  30. R. Kobayashi, J.A. Warren, and W.C. Carter: Vector-valued phase field model for crystallization and grain boundary formation. *Physica D* **119**, 415 (1998).
  31. T. Pusztai, G. Bortel, and L. Gránásy: Phase field theory of polycrystalline solidification in three dimensions. *Europhys. Lett.* **71**, 131 (2005).
  32. R. Kobayashi and J.A. Warren: Modeling the formation and dynamics of polycrystals in 3D. *Physica A* **356**, 127 (2005).
  33. R. Kobayashi and Y. Giga: Equations with singular diffusivity. *J. Stat. Phys.* **95**, 1187 (1999).
  34. J.A. Warren, R. Kobayashi, A.E. Lobkovsky, and W.C. Carter: Extending phase field models of solidification to polycrystalline materials. *Acta Mater.* **51**, 6035 (2003).
  35. A. Roy, J.M. Rickman, J.D. Gunton, and K.R. Elder: Simulation study of nucleation in a phase-field model with nonlocal interactions. *Phys. Rev. E* **56**, 2610 (1998).
  36. K.R. Elder, F. Drolet, J.M. Kosterlitz, and M. Grant: Stochastic eutectic growth. *Phys. Rev. Lett.* **72**, 677 (1994).
  37. M. Castro: Phase-field approach to heterogeneous nucleation. *Phys. Rev. B* **67**, 035412 (2003).
  38. A. Cacciuto, S. Auer, and D. Frenkel: Solid-liquid interfacial free energy of small colloidal hard-sphere crystals. *J. Chem. Phys.* **119**, 7467 (2003).
  39. Y. Mu, A. Houk, and X. Song: Anisotropic interfacial free energies of the hard-sphere crystal-melt interfaces. *J. Phys. Chem. B* **109**, 6500 (2005).
  40. G. Tóth: Investigation of crystal nucleation in the hard sphere system. Diploma Thesis Technical University of Budapest, Hungary (2004).
  41. S.L. Girshick and C.P. Chiu: Kinetic nucleation theory—A new expression for the rate of homogeneous nucleation from an ideal supersaturated vapor. *J. Chem. Phys.* **93**, 1273 (1990).
  42. L. Gránásy: Diffuse interface theory for homogeneous vapor condensation. *J. Chem. Phys.* **104**, 5188 (1996).
  43. J.H. Magill: Review spherulites: A personal perspective. *J. Mater. Sci.* **36**, 3143 (2001).
  44. F. Khoury: The spherulitic crystallization of isotactic polypropylene from solution: On the evolution of monoclinic spherulites from dendritic chain-folded precursors. *J. Res. Natl. Bur. Stand.* **70A**, 29 (1966).
  45. A. Keller and J.R. Waring: The spherulitic structure of crystalline polymers. Part III. Geometrical factors in spherulitic growth and the fine-structure. *J. Polymer Sci.* **17**, 447 (1955).
  46. J.H. Magill: Crystallization of poly-(tetramethyl-p-silphenylene)-solixane polymers. *J. Appl. Phys.* **35**, 3249 (1964).
  47. T. Pusztai, G. Bortel, and L. Gránásy: Phase field theory modeling of polycrystalline freezing. *Mater. Sci. Eng. A* **413–414**, 412 (2005).